

 Open access • Journal Article • DOI:10.1175/1520-0493(1992)120<0661:CMARTC>2.0.CO;2

## Cirrus microphysics and radiative transfer : cloud field study on 28 October 1986

— [Source link](#) 

Stefan Kinne, Thomas P. Ackerman, Andrew J. Heymsfield, Francisco P. J. Valero ...+2 more authors





**Institutions:** Ames Research Center, Pennsylvania State University, National Center for Atmospheric Research, University of Utah ...+1 more institutions

**Published on:** 01 May 1992 - Monthly Weather Review (American Meteorological Society)

**Topics:** Cirrus, Cloud cover, Cloud physics, Microphysics and Radiative transfer

Related papers:

- [The Relevance of the Microphysical and Radiative Properties of Cirrus Clouds to Climate and Climatic Feedback](#)
- [A parameterization of the particle size spectrum of ice clouds in terms of the ambient temperature and the ice water content](#)
- [Solar radiative transfer in cirrus clouds. I - Single-scattering and optical properties of hexagonal ice crystals. II - Theory and computations of multiple scattering in an anisotropic medium](#)
- [Influence of Cirrus Clouds on Weather and Climate Processes: A Global Perspective](#)
- [Role of small ice crystals in radiative properties of cirrus: A case study, FIRE II, November 22, 1991](#)

Share this paper:    

View more about this paper here: <https://typeset.io/papers/cirrus-microphysics-and-radiative-transfer-cloud-field-study-335cf4fej>

Cirrus Microphysics and Radiative Transfer :  
Cloud Field Study on October 28<sup>th</sup>, 1986

Stefan Kinne, NASA-Ames, MS 245-3, Moffett Field, CA 94035  
Thomas P. Ackerman, Dep.of Meteorology, Penn State, PA 16802  
Andrew J. Heymsfield, NCAR, P.O.Box 3000, Boulder, CO 80307  
Francisco P.J. Valero, NASA-Ames, MS 245-4, Mo.Field, CA 94035  
Kenneth Sassen, Dep.of Meteorology, Univ.of Utah, UT 84112  
James D. Spinhirne, NASA-Goddard, Greenbelt, MA 20771

## 1. INTRODUCTION

The radiative properties of cirrus clouds present one of the major unresolved problems in weather and climate research. Uncertainties in ice particle amount and size and, also, the general inability to model the single scattering properties of their usually complex particle shapes, prevent accurate model predictions. For an improved understanding of cirrus radiative effects, field experiments, as those of the Cirrus IFO of Fire, are necessary. Simultaneous measurements of (1) radiative fluxes and (2) cirrus microphysics at multiple cirrus cloud altitudes allow to pit calculated versus measured vertical flux profiles; with the potential to judge current cirrus cloud modeling.

## 2. MEASUREMENTS

As part of the detailed cirrus case study (Starr and Wylie, 1989), data are analyzed for a 75 by 50 km cirrus cloud field that moved over Wausau, WI, in the morning of October 28<sup>th</sup>, 1986. The observing systems provide simultaneous measurements of radiative broadband fluxes and cloud microphysics at altitudes of 6.1, 6.4, 7.0, 7.3, 7.6, 7.9 and 8.2km altitude within the cirrus cloud (NCAR King-air) and cloud geometry data from stratospheric (NASA ER-2) and groundbased (Wausau) remote sensing measurements. Trajectories of the two aircraft and the position of Wausau with respect to the moving cloud-field (78km/h 245°) in Figure 1 show that these measurements rarely occurred at the same cloud field position, so that flux profiles at cloud height from measurements are only realistic, if homogeneity of the cloud field can be guaranteed. Unfortunately, strong inhomogeneities are indicated by 10 $\mu$ m upwelling radiance measurements of the ER-2 and are illustrated by the contour plot of Figure 2. Equivalent blackbody temperatures of in the right half of the cloud field compared to those in the left half are lower by about 15K. Assuming an effective cloud altitude of 7.6km (240K atmospheric temperature), infrared optical depths larger than 2 for the right side and optical depths smaller than 1 for the left side of the cloud-field are detected. The groundbased lidar (Sassen, 1989) reveals an uniform cloud base at 6km altitude, while the ER-2 lidar (Spinhirne et al., 1989) detects cloud tops as high as 11km for the optically thicker right part of the cloud-field. Despite these cloud top heights, the chosen effective cloud altitude may even be lower than 7.6km (and optical depths larger), because

strong extinctions directly above the cloud base between 6.5 and 7.5km altitude generally dominate the radiative character of the cirrus cloud. The detected two natured character of the cloud-field is also supported by flux measurements, with solar and infrared optical depths of 5 and 3 for the right region being larger by a factor of 3 over those from the left cloud-field region. Thus, any comparison between measured and calculated fluxes has to treat both cloud-field domains separately.

### 3. MODELING

Calculations of broadband radiative fluxes are performed with an accurate 1-D spectral radiative transfer model. For the atmospheric profile, the 18 GMT Greenbay radiosonde data (Starr and Wylie, 1989), have been adjusted (T:-3K, water vapor saturation at cloud height) to make the sounding consistent with the King-air measurements. Humidity data above 11 km altitude and the ozone profile were taken from the US-Standard Atmosphere. Solar calculations assume a solar constant of  $1360 \text{ W/m}^2$  and a solar zenith angle of  $60^\circ$ . This angle is accurate to within a few degrees with respect to local time (10.30 - 11.30 am), latitude ( $45^\circ$ ) and time of year (October 28<sup>th</sup>). A solar surface albedo of 15% was adopted, which is typical of midlatitude land surfaces. The cloud is modeled in 300 km thick layers from the cloud base at 6.1km to 8.2km altitude in the optically thinner and to 10.6km altitude in the optically thicker region of the cloud-field. Single scattering properties for ice particles, which are compact crystals with branches, bullet rosettes and hollow-ended single columns in that order (Heymsfield et al., 1989), are derived from 2-D imaging probe data. First, columns and column rosettes are modeled from measurements of cross-section area and maximum particle dimension. Then these columnar shapes are expressed by spheres of equivalent surface area, which provide in Mie calculations almost identical extinctions. Non-spherical shape effects are accounted for by reducing the solar co-single scattering albedo of spheres to 0.7 of its original value and by reducing the solar asymmetry-factor by 0.05.

### 4. COMPARISON

The comparison between measured and calculated fluxes suffers from the inhomogeneity of the cloud-field. Measurements at the lower cloud altitudes occurred in the optically denser right section of the cloud-field (see Figure 1 and 2), while measurements above 7.5km altitude occurred in the optically thinner left section. This makes it difficult to establish an accurate radiative flux profile. Moreover, even within these regions for each cloud altitude a wide range of flux values is detected, especially at solar wavelengths. Since it is difficult to judge the accuracy for measurements in the optically thinner cloud region with measurements at only two cloud altitudes, the comparison, here, concentrates on results for the optically denser region of the cloud-field. Horizontal bars in Figure 3 indicate ranges of flux measurements in areas of the cloud-field,

where the equivalent blackbody temperature  $T_B$  (see Figure 2) dropped below 250K. To represent this cloud-field section in calculations, particle size distributions based on 2-D imaging probe averages from the five lowest flight legs between 6.1 and 7.5 km altitude have been modeled into a cloud layer between 6.1 and 10.6km altitude. These distributions are characterized by large crystals, since particles with equivalent radii of about 70 $\mu$ m provide the largest cross-section. However, there is an uncertainty towards smaller particle sizes with radii less than 20 $\mu$ m, the instrumentation was unable to detect. Assuming a decreasing particle density from 7.5km upward towards the cloud top, the total cloud optical depth amounts to 2.6. The comparison in Figure 3 shows that measurements indicate larger optical depths, especially at solar wavelengths. Even with the microphysics from region with  $T_B$  less than 240K the smallest solar downward fluxes cannot be reproduced. Since microphysical measurements might have overlooked a possible influence of small particles, additional small particles with radii of about 3 $\mu$ m in the water and in the ice phase have been added in two different cases to the detected average size distributions near the cloud base. Their addition certainly cloud explain the disagreement between calculated and measured fluxes.

## 5. Conclusion

Most of the problems in this study are linked to the inhomogeneity of the cloud-field. Thus, only studies on more homogeneous cirrus cloud cases promise a possibility to improve current cirrus parameterizations. Still, the current inability to detect small ice-particles will remains as a considerable handicap.

In future experiments an instrument is needed, that can detect concentrations of ice particles for sizes between 1 and 40 $\mu$ m. Most desirable in future experiments are measurements of microphysics and radiation, which are simultaneously taken at different cloud altitudes. Due to the lack of airborne instrumentation, however, measurements along altitude legs will generally be time delayed. Then a drift with the ambient air will make cloud measurements much more useful.

## REFERENCES

- Heymsfield, A.J. and K.M. Miller, 1989: October 27-28 1986 FIRE cirrus case study: Cloud microstructure.
- Sassen K. 1989: Wausau-lidar observations on October 28, 1986
- Spinhirne J.D. and W.D. Hart: ER-2 lidar and spectral radiometer cirrus observations for October 28, 1986.
- Starr D. and D.P. Wylie, 1989: The 27-28 October 1986 Fire case study: Meteorology and Cloud-Field.

all submitted to Mon.Wea.Rev.

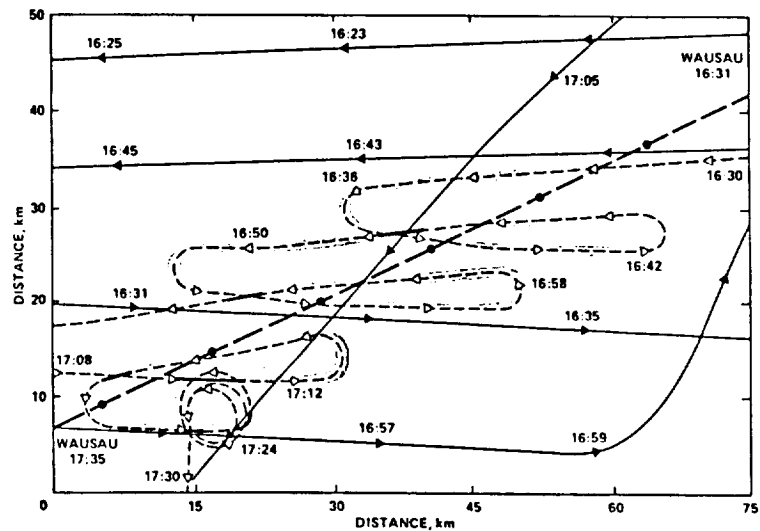


Figure 1 Analyzed 75 by 50 km cloud-field area. With respect to the movement of the cloud-field, the position of Wausau (dark dashed line, 10 min marks) and the trajectories of ER-2 (solid line, 2 min arrows) and King-air (shaded dashed line, 2 min arrows) are displayed. The King air climbed from 6.1km to 8.3km in seven constant altitude legs gaining altitude only  $180^{\circ}$  turns. The descent back to 6.1km occurred in a three loop spiral while drifting with ambient wind (displayed in the lower left corner).

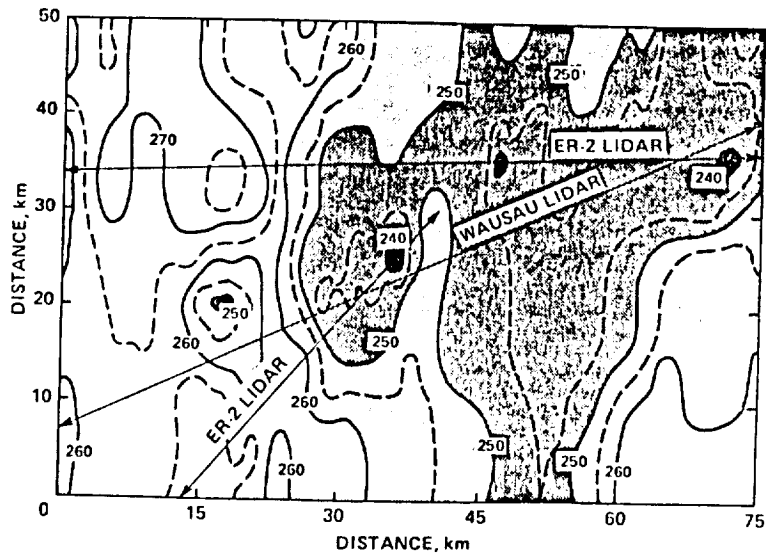


Figure 2 Contour plot of  $10\mu\text{m}$  equivalent blackbody temperatures as detected by the ER-2 at 19km altitude for the selected cloud-field area of Figure 1. Double arrow lines indicate the location of vertical cloud cross-sections by stratospheric (ER-2) and groundbased (Wausau) lidar measurements.

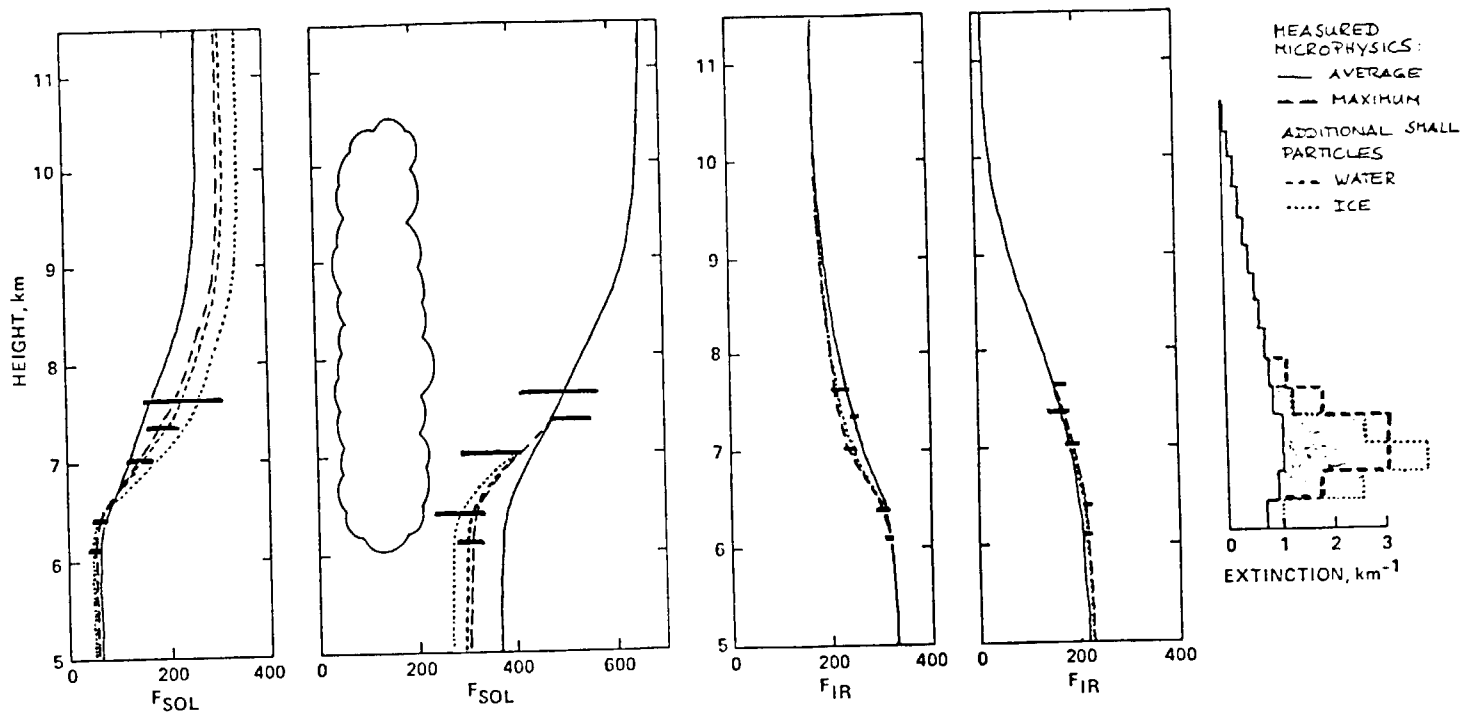


Figure 3 Comparison of measured and calculated broadband solar and infrared fluxes for the cloud-field section of large optical depths. Measurements (horizontal bars) are only available near the cloud base. Calculations (solid line,  $\tau:2.6$ ) are based on measured microphysical averages between the cloud base at 6.1 and 7.5 km altitude. Above 7.5 km a monotonically decreasing extinction was assumed towards the cloud top at 10.6 km (solid line). Also shown are results for microphysical maxima (long dashed line,  $\tau:4.4$ ) and calculations with added small particles in the water (short dashed line,  $\tau:4.9$ ) and ice-phase (dotted line,  $\tau:4.9$ ) near the cloud base. Also shown are the respective cloud extinctions at solar wavelengths, leading to the optical depths indicated above.

